a distribution of immediate environments for the aluminum atoms remaining in the framework. Comparison of parts b and c of Figure 2 shows that most, but not all, of the octahedral aluminum can be removed by washing subsequent to $SiCl_4$ treatment. Such octahedral aluminum that still remains may be neutralizing the negative framework charge brought about by the presence of tetrahedral aluminum. An ion-exchange equilibrium can be established during washing between Na^+ and $[Al(H_2O)_6]^{3+}$ competing for the cationic sites. Inspection of Figure 2c would suggest that most of the framework charge is neutralized by sodium and the remainder by $[Al(H_2O)_6]^{3+}$ (note that one octahedral Al atom balances the charge of *three* tetrahedral Al atoms). The poorer signal-to-noise ratio in Figure 2b,c in comparison with that of Figure 2a is due to the much lower concentration of aluminum in these samples. Another striking feature of the spectra in Figure 2 is the large change in the chemical shift of the tetrahedrally coordinated aluminum, 54.8 ppm in the dealuminated Na-Y as opposed to 61.3 ppm in the parent material. The origin of this effect is at present under investigation.

Acknowledgment. We acknowledge support from the Universities of Cambridge and Guelph and from the BP Research Centre, Sunbury. C.A.F. and J.S.H. acknowledge the financial support of the Natural Sciences and Engineering Research Council of Canada in the form of operating grants, and G.C.G. acknowledges the award of an NSERC Graduate Scholarship. The NMR spectra were obtained at the South-West Ontario High-Field NMR Facility (Dr. R. E. Lenkinski, Manager) funded by a Major Installation Grant from the NSERC.

Registry No. $SiCl_4$, 10026-04-7; ^{29}Si, 14304-87-1; Al, 7429-90-5.

Contribution from the Department of Chemistry, University of Iowa, Iowa City, Iowa 52242

Correlations of Axial Ligand Field Strength and Zero-Field Splittings in the Carbon-13 NMR Spectra of Five- and Six-Coordinate High-Spin Iron(III) Porphyrin Complexes

HAROLD M. GOFF,* ERIC T. SHIMOMURA, and MARTIN A. PHILLIPPI

Received April 12, 1982

Carbon-13 NMR spectra have been recorded for complexes of high-spin iron(III) porphyrins in which the axial anionic ligand has been varied. The $(Me_2SO)_2$ complexes of high-spin iron(III) tetraphenylporphyrins ((TPP)Fe^{III}) and natural-derivative porphyrins have also been examined. Replacement of a single anionic ligand with two solvent ligands induces striking changes in carbon-13 NMR spectra, with changes in the phenyl ortho-carbon and meso-carbon signals of (TPP)Fe^{III} on the order of several hundred ppm. This explains the seemingly anomalous upfield and downfield meso-proton shift values for five- and six-coordinate species. Results are interpreted in terms of unpaired spin delocalization through both σ- and π-type molecular orbitals, with a predominant π mechanism of Fe→porphyrin "back-bonding" in six-coordinate complexes. A contribution from porphyrin → Fe charge transfer places large unpaired spin density at the meso-carbon atom of five-coordinate species. Modulation of the meso-position spin density by differing axial anionic ligands is apparent in variable NMR chemical shift values for the phenyl and meso-carbon atoms of (TPP)FeX complexes. Phenyl shifts show a positive correlation with the zero-field splitting parameter, D, as measured by far-infrared and magnetic methods. A correspondence is also apparent between meso-carbon NMR shift values and Fe(III)/Fe(II) redox potentials. These observations suggest the ligand field strength of the axial ligand dictates the magnitude of unpaired spin density at the meso position, with larger downfield shifts associated with weaker field ligands. On this basis the following ordering of ligand field strength is offered for high-spin iron(III) porphyrins: $F^- > OPh^- > OPh(p\text{-}NO_2)^- > N_3^- \approx OAc^- > NCS^- > Cl^- > Br^- > I^-$.

Introduction

The high-spin state of iron(III) porphyrins results as a consequence of having either one or two weak-field ligands coordinated at the iron center. The best characterized five-coordinate species are those with a single anionic ligand, in which case the iron atom is raised typically 0.5 Å from the porphyrin plane.[1,2] The distorted-square-pyramidal environment serves to perturb the electronic properties of high-spin iron(III) particularly in the form of inducing large zero-field splitting. Coordination of extremely weak-field ligands such as perchlorate ion results in admixture of the $S = {}^3/_2$ state with the high-spin state.[3-5] Bisligated high-spin iron(III) porphyrin complexes may be generated through the action of weak-field coordinating solvents (i.e., dimethyl sulfoxide, tetramethylene sulfoxide, water, or alcohols) on certain five-coordinate adducts.[6-10] Core expansion allows placement of the iron atom in the plane of the porphyrin, and the resulting geometry about the iron center is one of pseudooctahedral symmetry. As such, the electronic properties of this six-coordinate complex might be expected to differ from those of the five-coordinate anion-bound derivative.

Both five-coordinate and six-coordinate high-spin iron(III) porphyrin prosthetic groups are found in hemoproteins. Examples include horseradish peroxidase, which seemingly has only a histidine axial ligand in the resting form, and metmyoglobin, which has histidine and water ligands.[11] It is therefore relevant to ask how mono- or bisligation, as well as the nature of the axial ligand(s), might influence the reactivity, electronic structure, and electron-transfer characteristics of high-spin iron(III) porphyrin complexes. Various physical techniques have been utilized in attempts to answer such

(1) Scheidt, W. R. In "The Porphyrins"; Dolphin, D., Ed.; Academic Press: New York, 1978; Vol. III, pp 463-511.
(2) Scheidt, W. R.; Reed, C. A. *Chem. Rev.* **1981**, *81*, 543.
(3) Dolphin, D. H.; Sams, J. R.; Tsin, T. B. *Inorg. Chem.* **1977**, *16*, 711.
(4) Reed, C. A.; Mashiko, T.; Bentley, S. P.; Kastner, M. E.; Scheidt, W. R.; Spartalian, K.; Lang, G. *J. Am. Chem. Soc.* **1979**, *101*, 2948.
(5) (a) Goff, H.; Shimomura, E. *J. Am. Chem. Soc.* **1980**, *102*, 31. (b) Boersma, A. D.; Goff, H. M. *Inorg. Chem.* **1982**, *21*, 581.
(6) Zobrist, M.; La Mar, G. N. *J. Am. Chem. Soc.* **1978**, *100*, 1944.
(7) Mashiko, T.; Kastner, M. E.; Spartalian, K.; Scheidt, W. R.; Reed, C. A. *J. Am. Chem. Soc.* **1978**, *100*, 6354.
(8) Budd, D. L.; La Mar, G. N.; Langry, K. C.; Smith, K. M.; Nayyir-Mazhir, R. *J. Am. Chem. Soc.* **1979**, *101*, 6091.
(9) Scheidt, W. R.; Cohen, I. A.; Kastner, M. E. *Biochemistry* **1979**, *18*, 3546.
(10) Morishima, I.; Kitagawa, S.; Matsuki, E.; Inubushi, T. *J. Am. Chem. Soc.* **1980**, *102*, 2429.
(11) (a) Spiro, T. G.; Stong, J. D.; Stein, P. *J. Am. Chem. Soc.* **1979**, *101*, 2648. (b) Rakshit, G.; Spiro, T. G. *Biochemistry* **1974**, *13*, 5317.

0020-1669/83/1322-0066$01.50/0

fundamental chemical questions. Among these, nuclear magnetic resonance spectroscopy has proven to be one of the most powerful for solution work at near-ambient temperatures. The large information content of the NMR spectrum appears by virtue of nuclear and electron spin interactions which yield greatly magnified nuclear chemical shift (isotropic shift) values. For the particular case of high-spin iron(III) complexes, proton NMR spectral line widths and dipolar shift have been shown to be sensitive to modulation of zero-field splitting by variation of the nature of axial anionic ligands.[12-15] Proton NMR spectroscopy was also first utilized to characterize bisligation in coordinating solvents,[6,16] and subsequent work has demonstrated diagnostic effects in the proton NMR spectra of five- and six-coordinate complexes.[8] Although instrumental limitations allowed only partial observation of signals in early studies,[17,18] carbon-13 NMR spectral measurements have now provided assignment of all possible resonances for five-coordinate complexes.[19-21] Likewise, due to severe signal broadening, location of all resonances for water-soluble (presumed) diaquo high-spin iron(III) porphyrin complexes remains incomplete.[22] Systematic carbon-13 NMR examination of five-coordinate complexes with a variety of anionic ligands is reported here. Results are interpreted in terms of zero-field splitting effects and spin-delocalization mechanisms. Explanation of seemingly anomalous proton NMR results for six-coordinate complexes[23] are readily understood by comparison of carbon-13 spectra. Results further provide strategy for label incorporation and observation of carbon-13 signals in hemoproteins.

Experimental Section

Iron porphyrin compounds were prepared by standard literature methods. Tetraphenylporphyrin (H_2TPP) and various phenyl-substituted derivatives were obtained by direct condensation of pyrrole with the appropriate benzaldehyde derivative in a propionic acid reflux.[24] Tetraphenylporphyrin with a carbon-13 label at the meso position was prepared with use of carbonyl-labeled benzaldehyde (60 atom %, Merck). Octaethylporphyrin (H_2OEP) was obtained via total pyrrole synthesis.[25] Iron insertion was performed under a nitrogen atmosphere in a dimethylformamide reflux with use of excess solid $FeCl_2$ (anhydrous, Alfa).[26] The solid iron(III) porphyrin obtained by addition of water to the cooled reaction mixture was purified by silica gel or alumina dry-column chromatography. Dichloromethane or chloroform containing 2–5% methanol was employed as eluting solvent. The μ-oxo dimeric iron(III) porphyrins were prepared from chloro derivatives by shaking a dichloromethane solution with aqueous 1 M NaOH solution followed by passage through a short basic alumina (Fisher) column using dichloromethane containing 2–5% methanol as an eluting solvent. Halide and acetate complexes were prepared by stirring methylene chloride or chloroform solutions of the μ-oxo dimer with the appropriate aqueous solution.[27,28] Crystalline products were generally isolated by slow addition of pentane or heptane during rotary evaporation of the chlorinated solvent. Thiocyanate and azide complexes were obtained via μ-oxo dimer cleavage using the appropriate aqueous sodium salt solution acidified with sulfuric acid.[27,29] Literature methods designed for preparation of natural-derivative iron porphyrin phenoxide complexes[30,31] were adapted for the $(TPP)Fe^{III}$ phenoxide and *p*-nitrophenoxide adducts. Iron(III) protoporphyrin dimethyl ester chloride was prepared by esterification of hemin chloride (Aldrich).[32] Nitrate and sulfate complexes were prepared from the μ-oxo dimer as previously described with use of 1 equiv of the appropriate acid.[21]

Isolated complexes were characterized by elemental analysis, thin-layer chromatography, visible–UV spectroscopy, and proton NMR

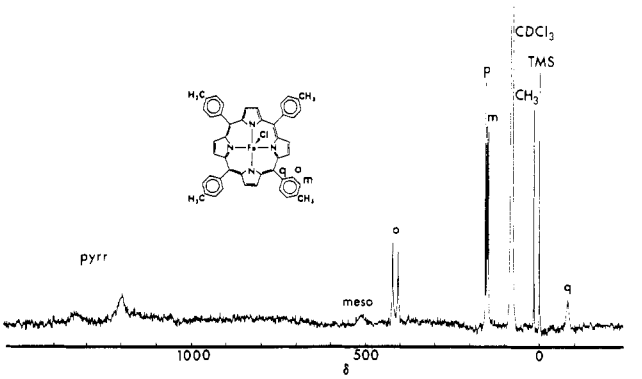

Figure 1. Carbon-13 NMR spectrum of TPP(*p*-CH_3)FeCl (iron porphyrin 0.05 M, $CDCl_3$ solvent, 30 °C, broad-band decoupled).

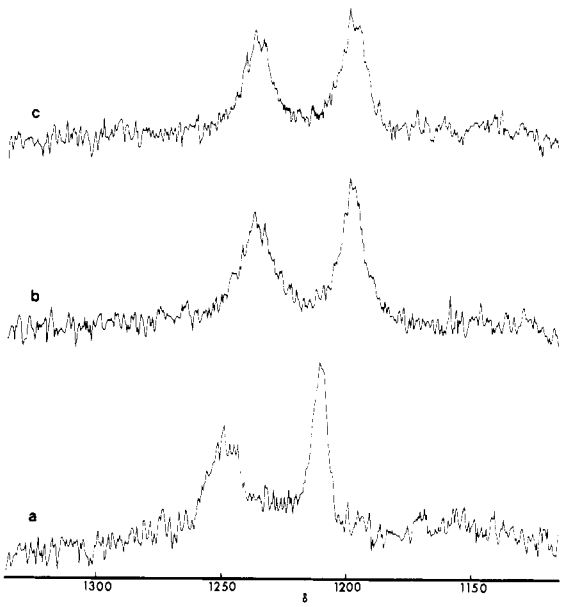

Figure 2. Far-downfield region for carbon-13 NMR spectrum of $((TPP)Fe)_2(SO_4)$ (iron porphyrin 0.05 M, $CDCl_3$ solvent): (a) proton-coupled spectrum, 26 °C; (b) off-resonance broad-band proton-decoupled spectrum, 30 °C; (c) broad-band decoupled spectrum where the proton irradiation frequency was placed at the 73-ppm pyrrole proton signal, 30 °C.

(12) Caughey, W. S.; Johnson, L. F. *J. Chem. Soc. D* **1969**, 1362.
(13) La Mar, G. N.; Eaton, G. R.; Holm, R. H.; Walker, F. A. *J. Am. Chem. Soc.* **1973**, *95*, 63.
(14) Walker, F. A.; La Mar, G. N. *Ann. N.Y. Acad. Sci.* **1973**, *206*, 328.
(15) Behere, D. V.; Birdy, R.; Mitra, S. *Inorg. Chem.* **1982**, *21*, 386.
(16) Kurland, R. J.; Little, R. G.; Davis, D. G.; Ho, C. *Biochemistry* **1971**, *10*, 2237.
(17) Goff, H. *Biochim. Biophys. Acta* **1978**, *542*, 348.
(18) Mispelter, J.; Momenteau, M.; Lhoste, J.-M. *J. Chem. Soc., Chem. Commun.* **1979**, 808.
(19) Phillippi, M. A.; Goff, H. M. *J. Chem. Soc., Chem. Commun.* **1980**, 455.
(20) Mispelter, J.; Momenteau, M.; Lhoste, J.-M. *J. Chem. Soc., Dalton Trans.* **1981**, 1729.
(21) Phillippi, M. A.; Baenziger, N.; Goff, H. M. *Inorg. Chem.* **1981**, *20*, 3904.
(22) Goff, H. M.; Morgan, L. O. *Bioinorg. Chem.* **1978**, *9*, 61.
(23) La Mar, G. N.; Walker, F. A. In "The Porphyrins"; Dolphin, D., Ed.; Academic Press: New York, 1979; Vol. IV, pp 61–157.
(24) Adler, A. D.; Longo, F. R.; Finarelli, J. D.; Goldmacher, J.; Assour, J.; Korsakoff, L. *J. Org. Chem.* **1967**, *32*, 476.
(25) Wang, C.-B.; Chang, C. K. *Synthesis* **1979**, *548*.
(26) Adler, A. D.; Longo, F. R.; Varadi, V. *Inorg. Synth.* **1976**, *16*, 213.
(27) Torrens, M. A.; Straub, D. K.; Epstein, L. M. *J. Am. Chem. Soc.* **1972**, *94*, 4162.
(28) Cohen, I. A.; Summerville, D. A.; Ru, S. R. *J. Am. Chem. Soc.* **1976**, *98*, 5813.
(29) Scheidt, W. R.; Summerville, D. A.; Cohen, I. A. *J. Am. Chem. Soc.* **1976**, *98*, 6623.
(30) Tang, S. C.; Koch, S.; Papefthymiou, G. C.; Foner, S.; Frankel, R. B.; Ibers, J. A.; Holm, R. H. *J. Am. Chem. Soc.* **1976**, *98*, 2414.
(31) Ainscough, E. W.; Addison, A. W.; Dolphin, D.; James, B. R. *J. Am. Chem. Soc.* **1978**, *100*, 7585.
(32) O'Keeffe, D. H.; Barlow, C. H.; Smythe, G. A.; Fuchsman, W. H.; Moss, T. H.; Lilienthal, H. R.; Caughey, W. S. *Bioinorg. Chem.* **1975**, *5*, 125.

Table I. Carbon-13 NMR Spectra of (TPP)FeX Derivatives[a]

anion	C atom						
	pyrr α	pyrr β	meso	quat	ortho	meta	para
F^-	1360[b]	1290[b]	353	−4	327, 319	143.8, 142.5	137.3
Cl^-	1200	1320	500	−70	416, 400	151.9, 147.9	142.3
Br^-	1170	1310	505	−77	430, 412	154.2, 149.4	143.8
I^-	1125	1270	478	−72	438, 412	157.2, 149.9	145.5
NCS^-	1200	1300	476	−64	393, 384	144.7, 142.1	165.0
N_3^-	1270	1300	433	−35	363, 353	145.1[c]	140.3
OAc^-	1310	1310	421	−33	365, 354	148.1, 145.1	139.5
OPh^-	1320[b]	1260[b]	381	−7	337, 324	143.4[c]	137.7
$OPh(p\text{-}NO_2)$	1330[b]	1280[b]	398	−17	344, 338	145.1, 144.2	139.0

[a] Conditions: $CDCl_3$ solvent, 30 °C, iron porphyrins 0.03–0.05 M, 1% $(CH_3)_4Si$. Downfield shifts are given a positive sign. [b] Assignments based on relative line widths. [c] Only one meta-carbon signal was observed (digital resolution 0.6 ppm).

spectroscopy. Although proton chemical shift values are similar for various high-spin (TPP)FeX complexes, trends in line widths[14,23] were useful in confirming the identity of the axial ligand. Carbon-13 NMR spectra reported here ultimately provided diagnostic criteria for integrity of complexes, in that contamination of product with μ-oxo dimer, chloride complex, or solvent of crystallization would have been readily apparent.

Proton and carbon-13 NMR spectra were recorded with JEOL FX-90Q and Bruker HX-90E pulsed Fourier transform spectrometers. Nearly saturated solutions (0.03–0.05 M) of iron(III) porphyrins in $CDCl_3$ were employed for carbon-13 spectroscopy. Both 10- and 5-mm NMR tubes were utilized. The sacrifice in sensitivity for the 5-mm tube was balanced by decreased line widths in proton-decoupled experiments as a consequence of diminished thermal gradients in the smaller volume sample. Unless noted otherwise, signals are referenced to internal Me_4Si and downfield shifts are given a positive sign.

Results

Assignment of Signals. Five-Coordinate Complexes. Complete assignment of carbon-13 signals in (TPP)FeCl and (TPP)FeI has recently been made by Mispelter et al. through incorporation of carbon-13 labels at the meso and pyrrole positions.[20,33] The natural-abundance carbon-13 spectrum of TPP(*p*-CH_3)FeCl is shown in Figure 1, and assignments are based on those presented earlier.[18-20] A surprising result is the assignment of the broader, further downfield pyrrole carbon signal to the pyrrole β-carbon atom.[20] This is the case for chloride and iodide complexes but is not necessarily true for all the derivatives examined here. The shift pattern can be demonstrated, however, through proton-decoupling experiments on a complex that exhibits rather sharp pyrrole signals. The far-downfield spectral region is shown in Figure 2 for the $((TPP)Fe)_2(SO_4)$ complex. Spectrum a represents the proton-coupled (decoupler off) case. The 150-Hz line width of the 1210-ppm signal approximates the C–H coupling constant, and the Lorentzian line shape of this signal therefore demonstrates that it does not represent a proton-bearing carbon. Both signals broaden and shift upfield approximately 12 ppm as proton-decoupling irradiation (spectrum b) is applied in a far-upfield region. This broadening is seemingly due to appearance of thermal gradients and a net 3.5 °C rise in temperature from dielectric heating. In spectrum c the decoupling frequency is applied at the 73-ppm pyrrole proton signal, resulting in decoupling and sharpening (330 to 270 Hz) of the pyrrole β-carbon signal at 1235 ppm. The assignment of pyrrole α- and β-carbon signals is thus independently confirmed for a non-halide high-spin iron(III) porphyrin complex.

Table I lists carbon-13 chemical shift values for nine anionic complexes of $(TPP)Fe^{III}$. Specific pyrrole carbon assignments must be considered tentative on the basis of the assumption that line widths parallel those observed for Cl^-, I^-, and SO_4^{2-}

(33) Note that tentative assignments made for meso and pyrrole carbons in ref 17 are incorrect.

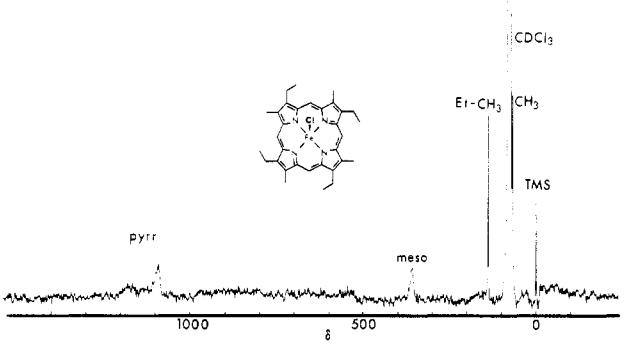

Figure 3. Carbon-13 NMR spectrum of (ETIO)FeCl (iron porphyrin ~0.02 M, $CDCl_3$ solvent, 51 °C, broad-band decoupled).

complexes. Carbon-13 chemical shift values have been previously reported for $(OEP)Fe^{III}$ complexes,[17] and the spectrum of the related (ETIO)FeCl species at 51 °C is shown in Figure 3. Assignments of pyrrole and meso-carbon signals follow those for (TPP)FeCl. The signal at 138.6 ppm approximates that of a signal for (OEP)FeCl in this region. Two signals are observed further upfield at 72.2 and 64.9 ppm when CH_2Cl_2 is employed (33 °C) to circumvent overlap of the solvent resonance. The 72.2-ppm signal matches one observed for (OEP)FeCl (74.4 ppm, CH_2Cl_2 solvent, 33 °C) and is assigned to the ring CH_2 group, whereas the 64.9-ppm signal is assigned to the ring CH_3 carbon atom. The 138.6-ppm resonance must therefore represent the ethyl CH_3 group. Natural-derivative iron(III) porphyrin spectra reveal no surprises with respect to the chemical shift patterns observed for (TPP)FeCl and (OEP)FeCl. The spectrum for (ProtDME)FeCl shown in Figure 4a is in agreement with the partial spectrum reported earlier,[17] with the exception of the meso-carbon assignment. Prior examination of various natural-derivative iron(III) porphyrin compounds and consideration of the (ETIO)FeCl spectrum serve to confirm assignments for CH_2, CH_3, and vinyl substituents.

Six-Coordinate Complexes. Addition of a coordinating solvent to a high-spin iron(III) complex containing a weakly coordinating anionic ligand results in displacement of the anionic ligand and biscoordination of solvent.[6-10,16] This is the case for iron(III) porphyrin nitrate species in dimethyl sulfoxide (Me_2SO) solvent or in a 2:1 $CDCl_3$–Me_2SO-d_6 solvent mixture. The proton NMR spectrum of $(TPP)FeNO_3$ in the 2:1 mixture (26 °C) exhibits a pyrrole proton signal at 66.8 ppm much as expected for the $(Me_2SO)_2$ complex at this temperature.[6] The corresponding carbon-13 spectrum appears in Figure 5. Assignment of the meso-carbon signal at 13 ppm (30 °C, 500-Hz line width) was made unequivocally by examination of the meso-labeled derivative. The 166.3-ppm signal is that of a quaternary carbon atom and is assigned to the quaternary phenyl carbon. The 127.4-ppm signal is assigned to the phenyl para-carbon atom on the basis of exam-

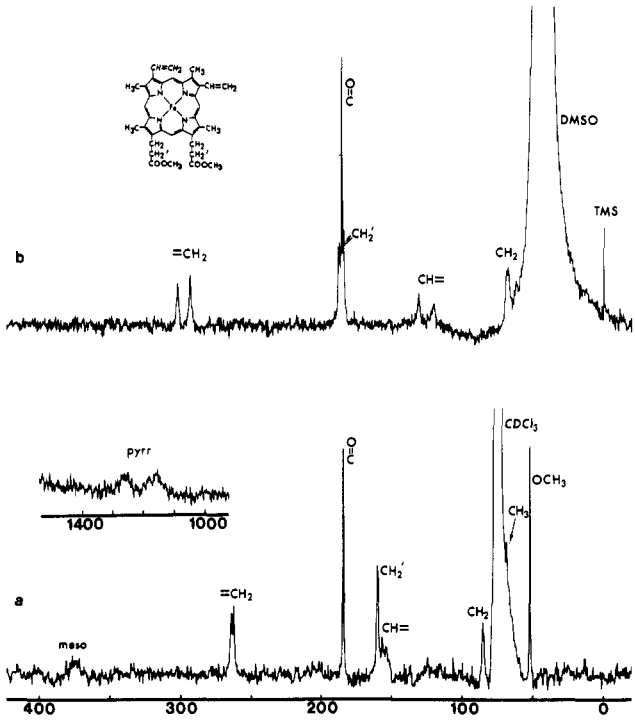

Figure 4. Carbon-13 NMR spectra of five- and six-coordinate complexes (iron porphyrins 0.05 M, 30 °C, broad-band decoupled): (a) (ProtDME)FeCl in $CDCl_3$; (b) (ProtDME)Fe$(Me_2SO)_2^+NO_3^-$ in Me_2SO-d_6.

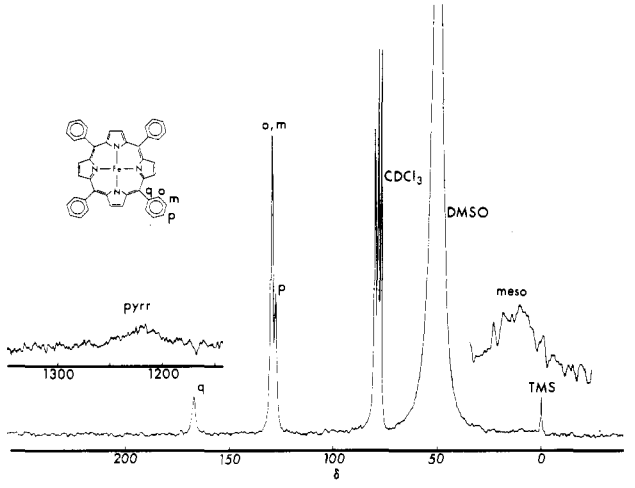

Figure 5. Carbon-13 NMR spectrum of (TPP)Fe$(Me_2SO)_2^+NO_3^-$ (iron porphyrin 0.05 M, 2:1 $CDCl_3$–Me_2SO-d_6, 30 °C, broad-band decoupled).

ination of the *p*-methyl analogue. A proton-coupled spectrum shows that the signal at 129.5 ppm represents proton-bearing carbon atoms. At −22 °C for a 9:1 $CDCl_3$–Me_2SO-d_6 solvent mixture, this signal is resolved into a relatively sharp component at 131.3 ppm, which must represent the meta-carbon atom, and a broader signal at 125.4 ppm, which is assigned to the ortho-carbon atom. Line broadening for the Me_2SO-d_6 carbon resonance suggests that solvent binding is in the near fast exchange limit. Hence, the broad signal at 1220 ppm must be assigned to a pyrrole carbon atom, and the other pyrrole signal is presumably too broad to detect with available instrumentation.

A partial carbon-13 spectrum is shown in Figure 4b for the $(Me_2SO$-$d_6)_2$ adduct of (ProtDME)Fe^{III}. Shift patterns for pyrrole substituents are much like those of the corresponding chloride complex. Significant changes do occur for chemical shift values of side-chain substituents in that resonances for carbon atoms attached directly to the ring move upfield, whereas a downfield bias is observed for resonances of carbon atoms β to the ring.

Discussion

The potential utility of carbon-13 NMR spectroscopy for monitoring perturbations of metalloporphyrin electronic and magnetic environments is apparent from listings in Table I. In particular, certain resonances are quite sensitive to the nature of the axial anionic ligand. Corresponding proton NMR spectra of the various complexes show more subtle changes in line width and chemical shift values,[15,23] and the broad phenyl ortho-proton signals are not generally resolved. The greater dispersion of carbon-13 spectra permits ready observation of phenyl ortho-carbon signals. Variation in the zero-field splitting parameters, D, is seemingly responsible for line width changes in proton spectra of several iron(III) porphyrin anion complexes.[12-15] Dipolar shifts for the otherwise magnetically isotropic d^5 high-spin iron(III) center are presumably induced through a zero-field splitting mechanism.[12-15] Values of D have been measured directly by far-infrared spectroscopy[34,35] and by curve fitting of variable-temperature single-crystal magnetic measurements.[36] The order of D values for the respective iron(III) porphyrin complexes follows: (TPP)FeX, $D_{NCS^-} < D_{Cl^-} < D_{Br^-} < D_{I^-}$;[36] iron(III) deuteroporphyrin dimethyl ester, $D_{F^-} < D_{N_3^-} < D_{Cl^-} < D_{Br^-} < D_{I^-}$;[34] iron(III) protoporphyrin dimethyl ester, $D_{F^-} < D_{Cl^-} < D_{N_3^-} < D_{I^-}$.[34,35] Reversal of the $D_{N_3^-}$, D_{Cl^-} order for the last two iron porphyrins indicates the dependence of D values on porphyrin structure.

Correlations exist between D values and chemical shifts for certain carbon atoms of (TPP)FeX complexes, and these correlations involve contact as well as dipolar contributions. Calculations based on D values show that carbon-13 dipolar shifts should be less than 40 ppm (pyrrole α-carbon) for the five-coordinate high-spin iron(III) complexes studied here.[20] Examination of Table I reveals ordering of certain carbon-13 resonance values in common with the D values for (TPP)FeX and iron(III) deuteroporphyrin dimethyl ester. Thus, chemical shift values for the (average) phenyl ortho-carbon and pyrrole α-carbon signals follow the order shown by the following: ortho carbon, $\delta_{F^-} < \delta_{N_3^-} < \delta_{NCS^-} < \delta_{Cl^-} < \delta_{Br^-} < \delta_{I^-}$; α-carbon, $\delta_{F^-} > \delta_{N_3^-} > \delta_{NCS^-} \approx \delta_{Cl^-} > \delta_{Br^-} > \delta_{I^-}$. With the exception of the iodide complex, the meso-carbon and quaternary phenyl carbon resonance values are also ordered with the zero-field splittings. The anomalous behavior of the iodide complex may well be due to the high degree of covalency reported for the Fe–I bond.[37]

The correspondence between isotropic shifts and zero-field splittings does not necessarily imply that large contact shifts are modulated by the D value. This behavior most likely suggests a common factor controlling both the zero-field splitting and the magnitude of unpaired spin delocalization. Examination of structural parameters[1,2,21] showed no apparent relation between the magnitude of isotropic shifts and Fe–pyrrole nitrogen bond lengths or iron displacement from the porphyrin plane. The ordering of ligands in nephelauxetic or spectrochemical series[38] parallels in part the ordering of iso-

(34) (a) Brackett, G. C.; Richards, P. L.; Caughey, W. S. *J. Chem. Phys.* **1971**, *54*, 4383. (b) Richards, P. L.; Caughey, W. S.; Eberspaecher, H.; Feher, G.; Malley, M. *Ibid.* **1967**, *47*, 1187.
(35) Uenoyama, H. *Biochim. Biophys. Acta* **1971**, *230*, 479.
(36) (a) Behere, D. V.; Marathe, V. R.; Mitra, S. *J. Am. Chem. Soc.* **1977**, *99*, 4149. (b) Behere, D. V.; Mitra, S. *Inorg. Chem.* **1979**, *18*, 1723. (c) Behere, D. V.; Date, S. K.; Mitra, S. *Chem. Phys. Lett.* **1979**, *68*, 544. (d) Behere, D. V.; Birdy, R.; Mitra, S. *Inorg. Chem.* **1981**, *20*, 2786.
(37) Pasternack, M.; Debrunner, P. G.; DePasquali, G.; Hager, L. P.; Yoeman, L. *Proc. Natl. Acad. Sci. U.S.A.* **1970**, *66*, 1142.
(38) Huheey, J. E. "Inorganic Chemistry"; 2nd ed.; Harper and Row: New York, 1978; pp 361, 391.

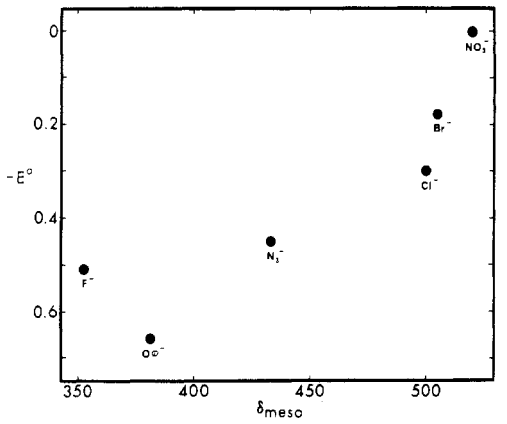

Figure 6. Plot of the reduction potentials for Fe(III) → Fe(II) for (TPP)FeX vs. the observed meso-carbon resonance values at 30 °C. Reduction potentials were measured by cyclic voltammetry and referenced to the SCE.[21,39,40]

tropic shift values, but notable deviations are apparent. A correlation seemingly exists between isotropic shift values and iron(III) → iron(II) redox potentials. Figure 6 serves to demonstrate the correspondence (not necessarily linear) through comparison of the meso-carbon chemical shift value and available potentials as measured by cyclic voltammetry. Redox potentials measured in this laboratory are consistent with those reported in the literature.[21,39,40] The iron(III) reduction potential provides a relative measure of ligand affinity for the iron(III) vs. the iron(II) state. Thus, if the affinity for iron(II) is constant among the ligands in Figure 6, the decrease in $E°$ values from NO_3^- to OPh^- must reflect more thermodynamically favorable ligand binding for the iron(III) complex. Deviation in the chemical shift vs. redox potential pattern might be anticipated for the fluoride ion, as this ligand does show significant affinity for the iron(II) state.[39]

Perturbations of zero-field splitting, redox properties, and magnitudes of unpaired spin delocalization (as measured by NMR) seemingly reflect the strength of axial ligand interaction. The value of D is thought to depend on the axial ligand field strength, with a smaller zero-field splitting indicating a stronger axial ligand interaction.[36] The demonstrated correspondence between selected carbon-13 NMR resonance positions and the order of D values thus suggests that the NMR spectrum is determined to a large extent by the axial ligand field strength. The average phenyl ortho-carbon resonance value appears to provide the most reliable correspondence with known zero-field splittings. Thus, on the basis of average phenyl ortho-carbon isotropic shifts, the following ordering of ligand field strength is offered for five-coordinate, high-spin (TPP)FeX: $F^- > OPh^- > OPh(p\text{-}NO_2)^- > N_3^- \approx OAc^- > NCS^- > Cl^- > Br^- > I^-$. Entries could also be made for bridged SO_4^{2-} and NO_3^-, but this may be presumptive given the bidentate character of these ligands.[21]

For a better understanding of patterns of carbon-13 chemical shifts, comparisons have been made for the observed values of the meso-carbon atom vs. those of the phenyl ortho-, quaternary phenyl, pyrrole α-, and pyrrole β-carbon atoms. Data from Table I along with literature values for nitrate and sulfate complexes[21] are utilized. Plots in Figures 7 and 8 appear to be linear, although there is no compelling reason that this should be the case. It is not surprising that a correlation should exist between shifts for the meso-carbon atom and attached phenyl carbon atoms. Significant shifts, alternating in spin, for the quaternary and phenyl ortho-carbon atoms must result

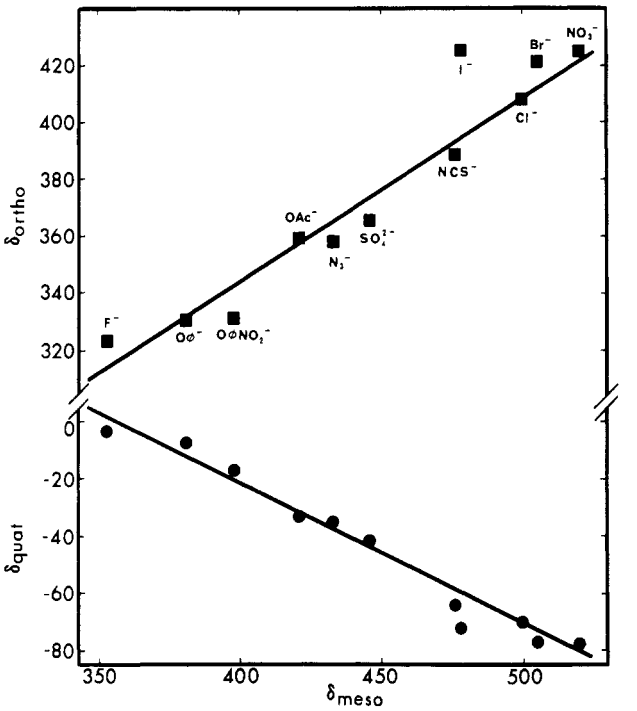

Figure 7. Plots of observed phenyl carbon-13 NMR signals vs. the meso-carbon signal of (TPP)FeX ($CDCl_3$ solvent, 30 °C).

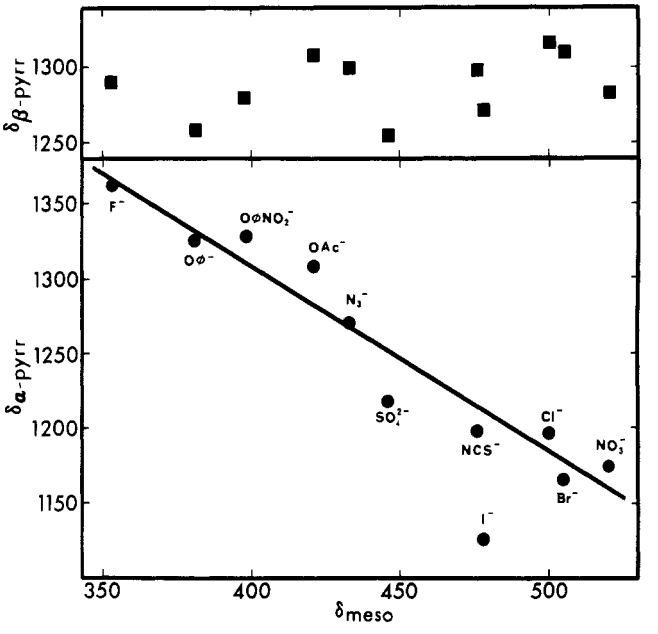

Figure 8. Plots of observed pyrrole carbon-13 NMR signals vs. the meso-carbon signal of (TPP)FeX ($CDCl_3$ solvent, 30 °C).

from large π spin density at the meso-carbon atom and an associated π–σ spin polarization mechanism. An argument is made for predominant π vs. σ spin density at the meso-carbon atom based on the alternation in sign of quaternary and ortho phenyl shifts and an upfield-shifted meso-proton signal. Attaching a stronger field ligand such as fluoride ion serves to diminish the spin density at the meso-carbon atom. In the extreme case where two axial Me_2SO ligands are bound (Figure 5), the meso-carbon signal is actually shifted upfield of the diamagnetic reference value to 13 ppm. Quaternary and phenyl ortho-carbon resonances are likewise drastically affected, but correlations with the meso-carbon resonance are amazingly preserved. If the plots in Figure 7 are extrapolated to include the 13-ppm meso-carbon resonance of (TPP)Fe-$(Me_2SO)_2^+$, the corresponding quaternary and ortho-carbon

(39) Bottomley, L. A.; Kadish, K. M. *Inorg. Chem.* **1981**, *20*, 1348.
(40) Phillippi, M. A.; Shimomura, E. T.; Goff, H. M. *Inorg. Chem.* **1981**, *20*, 1322.

Table II. Electron Densities for Possible π Molecular Orbitals[a]

π MO	meso C	pyrr α-C	pyrr β-C	N
3e(π)	0	0.0173	0.0625	0.0905
4e(π^*)	0.1034	0.0156	0.0350	0.0453

[a] Values represent linear combinations of the two e orbitals and are normalized to one electron per porphyrin (taken from ref 43).

resonance values are 171 and 95 ppm. These "expected" results are to be compared with respective values of 166 and 129.5 ppm. The correspondence is almost uncanny, given the out-of-plane iron configuration of anionic complexes vs. the pseudooctahedral configuration of the $(Me_2SO)_2$ adduct.

An inverse correspondence exists between shifts for the meso-carbon atom and those of the pyrrole α-carbon atom as shown in Figure 8. Thus, as stronger ligands diminish the meso-carbon shift value, the pyrrole α-carbon shift increases. Extension of this correlation to the Me_2SO complex is not productive, as we have not yet detected and assigned both pyrrole carbon signals of the six-coordinate species. It should be noted that a simple correlation is not apparent between meso-carbon and pyrrole β-carbon shifts.

A reasonable explanation for the inverse correlation of meso- and pyrrole α-carbon shifts has been provided by Mispelter et al.[20] on the basis of a comparison of (TPP)FeCl and (TPP)FeI spectra. Significant π spin density serves to polarize the spin at an adjacent carbon atom and thus exerts an upfield bias. Reduction of π spin density at the meso-carbon atom would reduce the upfield bias at the pyrrole α-carbon atom and thus make the downfield shift by a predominant σ spin delocalization more apparent.

Unpaired spin density may be delocalized through either σ-type or π-type porphyrin MO's. Both mechanisms are seemingly operative for high-spin iron(III) porphyrin complexes, as both σ-symmetry $d_{x^2-y^2}$ and π-symmetry d_{xz}, d_{yz} orbitals are half-filled. Direct delocalization of σ spin density results in downfield shifts. Positive π spin density is normally associated with downfield carbon-13 shifts, although an upfield ligand-centered dipolar term and polarization by spin density on neighboring carbon atoms may provide a net upfield shift.[41,42] Hückel calculations reveal that two sets of π MO's are energetically available for interaction with the e orbital set (d_{xz}, d_{yz}). The 3e(π) set is filled (bonding), whereas the 4e(π^*) set is vacant (antibonding).[43] The average electron distributions (normalized to one unpaired electron per porphyrin) are described in Table II. This listing suggests a very large downfield shift for the meso-carbon atom in the limit of a metal→4e(π^*) "back-bonding" mechanism and little shift at this position for a metal ← 3e(π) charge-transfer mechanism. Bisligated high-spin iron(III) porphyrins appear to fit the latter category, much as is the case for low-spin iron(III) complexes.[23,42] Although meso-carbon atoms exhibit sizable downfield shifts, the magnitude of these values should exceed those for the β-carbon atom in the limit of a 4e(π^*) delocalization mechanism. The fact that meso-carbon shifts for five-coordinate complexes do not fit either limit for π delocalization has been noted previously.[20] One possible explanation for this behavior would bring into question the numerical validity of average electron distributions and perhaps the identity of HOMO's and LUMO's for five-coordinate metalloporphyrin complexes showing considerable doming to accommodate a distorted-square-pyramidal metal environment. Alternatively, a mixing of the closely spaced 3e(π) and 4e(π^*) MO's could account for the variable meso-carbon π spin delocalization as the axial ligand is changed. Whatever the π spin delocalization mechanism, a progression of values is apparent for anionic ligands of varying binding affinity. Porphyrin structure is important in this regard, as the meso-carbon signal for (TPP)FeCl is some 120 ppm further downfield than that for (OEP)FeCl.

Results of self-consistent-charge extended Hückel calculations[44] for high-spin iron(III) porphyrins must be discussed in context with experimental results presented here. The theoretical calculations predict an unpaired spin population at the pyrrole α-carbon atom for the halide complexes in the order $F^- > Cl^- > Br^- > I^-$. This is consistent for the ordering of pyrrole α-carbon shifts seen in Figure 8. Calculations predict the same ordering of unpaired spin population for pyrrole β- and meso-carbon signals. The scatter of pyrrole β resonances in Figure 8 precludes comparison of theoretical and experimental results. However, the predicted and observed orderings for the meso-carbon atom are clearly in opposite directions, with the meso-carbon shift considerably greater for the iodide vs. the fluoride complex. Hopefully the data presented here will be employed in a semiempirical approach to provide a better theoretical description of spin density profiles.

Acknowledgment. We gratefully acknowledge support from the National Science Foundation, NSF Grant CHE 79-10305.

Registry No. (TPP)FeF, 55428-47-2; (TPP)FeCl, 16456-81-8; (TPP)FeBr, 25482-27-3; (TPP)FeI, 25482-28-4; (TPP)FeNCS, 25482-29-5; (TPP)FeN_3, 51455-98-2; (TPP)FeOAc, 33393-26-9; (TPP)FeOPh, 76282-28-5; (TPP)FeOPh(p-NO_2), 83486-39-9; TPP(p-CH_3)FeCl, 19496-18-5; ((TPP)Fe)$_2(SO_4)$, 72895-19-3; (ETIO)FeCl, 19413-49-1; (ProtDME)FeCl, 15741-03-4; (ProtDME)Fe$(Me_2SO)_2^+NO_3^-$, 83477-05-8; (TPP)Fe$(Me_2SO)_2^+$-NO_3^-, 83540-93-6.

(41) Karplus, M.; Fraenkel, G. K. *J. Chem. Phys.* **1961**, *35*, 1312.
(42) Goff, H. M. *J. Am. Chem. Soc.* **1981**, *103*, 3714.
(43) (a) Longuet-Higgins, H. C.; Rector, C. W.; Platt, J. R. *J. Chem. Phys.* **1950**, *18*, 1174. (b) Zerner, M.; Gouterman, M.; Kobayashi, H. *Theor. Chim. Acta* **1966**, *6*, 363.
(44) Mun, S. K.; Mallick, M. K.; Mishra, S.; Chang, J. C.; Das, T. P. *J. Am. Chem. Soc.* **1981**, *103*, 5024.